GEOLOGY | THE GEOLOGICAL SOCIETY OF AMERICA®

https://doi.org/10.1130/G48486.1

Manuscript received 6 October 2020
Revised manuscript received 20 December 2020
Manuscript accepted 24 December 2020

Published online 22 February 2021

Subduction erosion and crustal material recycling indicated by adakites in central Tibet

Zong-Yong Yang[1,2,3,4], Qiang Wang[1,2,4]*, Lu-Lu Hao[1], Derek A. Wyman[5], Lin Ma[1], Jun Wang[1,2], Yue Qi[1,2], Peng Sun[1,4] and Wan-Long Hu[1,4]

[1]State Key Laboratory of Isotope Geochemistry, Guangzhou Institute of Geochemistry, Chinese Academy of Sciences, Guangzhou 510640, China
[2]CAS Center for Excellence in Deep Earth Sciences, Guangzhou 510640, China
[3]State Key Laboratory of Ore Deposit Geochemistry, Institute of Geochemistry, Chinese Academy of Sciences, Guiyang 550081, China
[4]College of Earth and Planetary Sciences, University of the Chinese Academy of Sciences, Beijing 100049, China
[5]School of Geosciences, The University of Sydney, Camperdown, New South Wales 2006, Australia

ABSTRACT

Subduction erosion is important for crustal material recycling and is widespread in modern active convergent margins. However, such a process is rarely identified in fossil convergent systems, which casts doubt on the importance of subduction erosion through the geological record. We report on ca. 155 Ma Kangqiong (pluton) intrusive rocks of a Mesozoic magmatic arc in the southern Qiangtang terrane, central Tibet. These rocks mainly consist of trondhjemites and tonalites and are similar to slab-derived adakites with mantle-like zircon oxygen isotope compositions ($\delta^{18}O$ = 5.2‰–5.6‰), they display more evolved Sr-Nd isotopes and higher Th/La relative to mid-oceanic ridge basalts from the Bangong-Nujiang suture, and they contain abundant amphibole and biotite. These characteristics indicate magma generation via H_2O-fluxed melting of eroded forearc crust debris with subducted oceanic crust at 1.5–2.5 GPa and 700–800 °C. In addition, the intrusions are exposed <20 km north of the Bangong-Nujiang suture. Given the formation of adakites, narrow arc-suture distance, migration of the Jurassic frontal arc toward the continent interior, and other independent geological archives, we suggest that the hydrated forearc crust materials were removed from the overlying plate and carried into the mantle by subduction erosion. Our study provides the first direct magmatic evidence for a subduction erosion process in pre-Cenozoic convergent systems, which confirms an important role for such processes in subduction-zone material recycling.

INTRODUCTION

Continental crust may be recycled primarily in active subduction zones by subduction erosion (Scholl et al., 1980; von Huene et al., 2004; Clift et al., 2009; Vannucchi et al., 2013), a process involving large positive topographic relief on the descending slab (von Huene et al., 2004), identified by geophysical (seismic) imaging, distinctive arc rocks, and the characteristics of certain sedimentary rocks (Ranero and von Huene, 2000; Vannucchi et al., 2013). During subduction erosion, at least part of the arc crust removed from the overlying plate may be involved in melting, and ultimately reincorporated into the crust via arc magmatism (Stern and Kilian, 1996; Kay et al., 2005; Goss et al., 2013; Straub et al., 2020). Subduction erosion also results in the truncation and slope deformation of forearc crust (Ranero and von Huene, 2000), rapid forearc basin subsidence (Vannucchi et al., 2013), secular renewal of sediment provenance (Grove et al., 2008), and frontal arc migration (Kay et al., 2005; Goss et al., 2013). Consequently, subduction erosion is critical for crust recycling (von Huene et al., 2004; Clift et al., 2009).

However, subduction erosion is not easily identified in fossil convergent systems, largely due to the lack of evidence of the topographic characteristics of the underthrust slab. No Paleozoic to Mesozoic magmatic rocks related to subduction erosion have yet been verified convincingly, although some Cenozoic adakites in arc settings are considered to have a genetic relationship with this process (Kay et al., 2005; Goss et al., 2013). We report the first direct magmatic evidence for a similar process in pre-Cenozoic convergent systems in central Tibet. This suggests that subduction erosion was significant for arc crust recycling in the Phanerozoic.

GEOLOGICAL SETTING AND ROCKS

The Bangong-Nujiang suture (BNS; Figs. 1A and 1B) in central Tibet separates the southern Qiangtang terrane (SQT) from the Lhasa terrane (LT) (Zhu et al., 2016). Oceanic slab subduction beneath the SQT along the BNS likely initiated at ca. 170 Ma (Zhu et al., 2016). Terrane assembly probably occurred at ca. 140 Ma (Zhu et al., 2016) or later (Kapp et al., 2007; Hao et al., 2019).

The Jurassic Kangqiong pluton (Fig. 1C), part of a Mesozoic magmatic arc in the SQT, is located <20 km from the BNS (Li et al., 2016). It comprises mainly equigranular to porphyritic trondhjemites and tonalites consisting of plagioclase, quartz, pyroxene, amphibole, and biotite (Fig. S1 in the Supplemental Material[1]) and small fine-grained granite bodies.

RESULTS

The Kangqiong pluton was generated in the Late Jurassic. Secondary ion mass spectrometry zircon U-Pb isotopic results (Fig. S2) gave mean

*E-mail: wqiang@gig.ac.cn

[1]Supplemental Material. Supplemental figures, analytical methods and results, and data and results tables. Please visit https://doi.org/10.1130/GEOL.S.13708522 to access the supplemental material, and contact editing@geosociety.org with any questions.

CITATION: Yang, Z.-Y., et al., 2021, Subduction erosion and crustal material recycling indicated by adakites in central Tibet: Geology, v. 49, p. 708–712, https://doi.org/10.1130/G48486.1

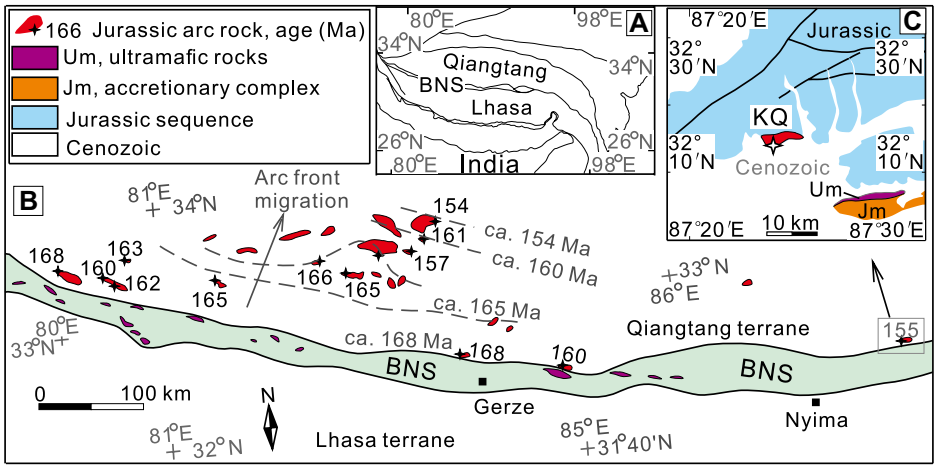

Figure 1. (A) Tectonic map of the Tibetan Plateau. (B) Simplified map showing Jurassic magmatic arc rocks in the southern Qiangtang terrane (modified after Zhu et al., 2016). Dashed gray lines represent the arc front. (C) Geology of the Kangqiong pluton (KQ) area. Blue area is the Jurassic sequence, and white area is the Cenozoic deposit. BNS—Bangong-Nujiang suture.

ages of 154.6 ± 1.6 Ma and 153.1 ± 2.6 Ma for the Kangqiong trondhjemites-tonalites and granites, respectively.

The trondhjemites and tonalites have a narrow range of SiO_2 (64.2–68.2 wt%) and K_2O (1.58–2.89 wt%; Fig. S3A), are sodium rich (Fig. 2A), and have variable MgO (1.48–3.23 wt%) and Mg# (41–69; Fig. S3B). They have arc-like trace element features (Figs. S3C and S3D) with fractionated rare earth element (REE) patterns (La/Yb = 8.12–24.7), high Sr contents (>460 ppm), low heavy REE (HREE) and Y contents (<13.3 ppm), negligible Eu anomalies (Eu/Eu* [chondrite-normalized Eu/$\sqrt{(Sm \times Gd)}$] = 0.85–1.11) (Fig. S3C), and elevated Sr/Y ratios (>40; Fig. 2B) relative to common arc rocks. These features resemble those of typical adakites (Drummond et al., 1996); hence, these rocks are referred to here as Kangqiong adakites (KQAs). Granite samples have higher SiO_2 (>72.0 wt%), lower Sr/Y (<40), and slightly negative Eu anomalies (Fig. S3C).

The KQAs have variable initial $^{87}Sr/^{86}Sr$ ratios (0.7050–0.7072) and Nd isotope compositions ($\varepsilon_{Nd(t)}$ = −0.79 to +1.95) (Fig. S4). The granites have more evolved Sr-Nd isotope compositions than KQAs. The KQAs and granites have mantle-like zircon oxygen isotope compositions of 5.6‰ ± 0.5‰ and 5.4‰ ± 0.6‰ (2 standard deviations [SD]), respectively (Fig. 2C).

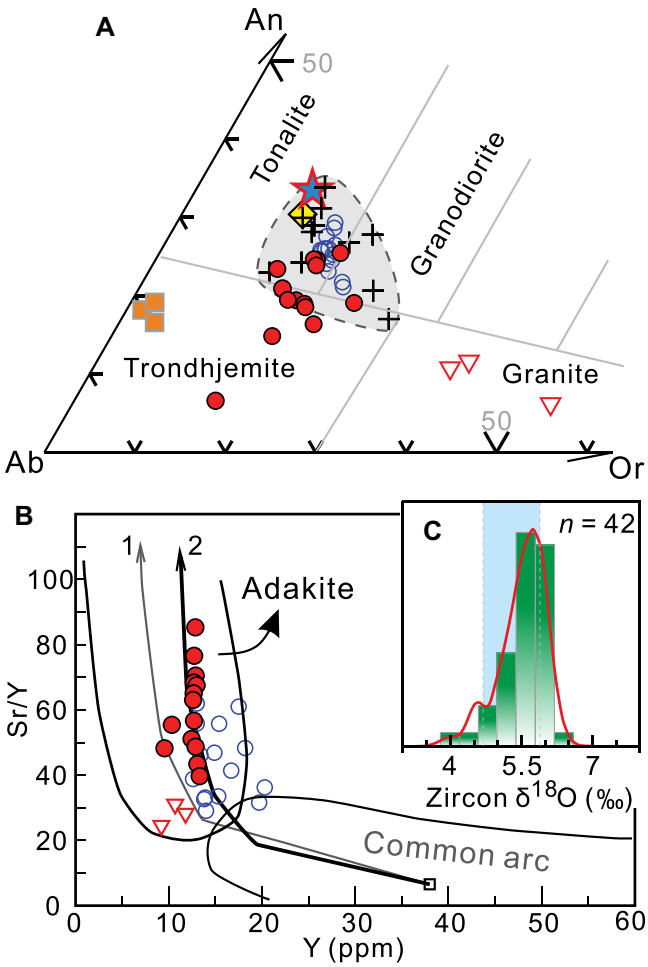

Figure 2. (A) CIPW (Cross, Iddings, Pirsson, and Washington) normative albite-anorthite-orthoclase (Ab-An-Or) plot. Filled circles (this study) and open circles (Li et al., 2016) are Kangqiong (KQ; Tibet) adakites, and inverted triangles are KQ granites. The average of Mount Pinatubo (Philippines) adakites (diamond) and phase equilibria experimental melts (cross and dashed gray field) are from Prouteau et al. (1999); star denotes average of Cenozoic adakites (Drummond et al., 1996); trondhjemitic pegmatites (square) are from the Catalina Schist (Southern California, USA; Sorensen, 1988). Dashed gray field is defined by the phase equilibria melts (cross) of Prouteau et al. (1999). (B) Sr/Y versus Y plot (modified after Drummond et al., 1996). Curves 1 and 2 refer to partial melt trends of mid-oceanic ridge basalt (MORB) leaving eclogite (1) or garnet amphibolite (2) restite. (C) Histograms (green bars) and probability density line (red line) of zircon oxygen (O) isotopic compositions of the KQ puton. Blue bar denotes the oxygen isotopic composition range of normal mantle.

DISCUSSION

Genesis of Kangqiong Adakites

Models for adakite genesis include (1) partial melting of oceanic slab (Drummond et al., 1996); (2) partial melting of thickened, delaminated, or subducted continental crust (Wang et al., 2008); and (3) fractional crystallization of mafic magmas (Castillo et al., 1999). The KQAs could have been generated by model 1, as explained below.

A previously hypothesized Middle Jurassic SQT-LT collision was based mainly on an angular unconformity in the northeastern Nyima area of Tibet (Fig. 1B; Ma et al., 2017). However, its significance is ambiguous (Ma et al., 2017): Jurassic sediments in the SQT show no distinctive LT sedimentary provenance, indicating that no exotic component entered the trench, and no fossil or absolute age constraints exist for this unconformity. In fact, recent tectonic, sedimentary, magmatic, and paleomagnetic data suggest the Bangong-Nujiang Ocean was still open during the Middle to Late Jurassic and closed during the Early Cretaceous (Hao et al., 2019; Kapp and DeCelles, 2019; Lai et al., 2019; Cao et al., 2020), indicating the ca. 155 Ma KQAs were generated in an arc setting.

Because model 2 commonly occurs in post-collisional, or within-plate, settings, it may be safely excluded. Moreover, the KQAs have lower K_2O, higher Mg# (Fig. S3A and S3B), and higher $\varepsilon_{Nd(t)}$ values than continental crust–derived adakitic rocks (Fig. S4). A slightly positive correlation between initial $^{87}Sr/^{86}Sr$ and MgO (Fig. S6C) is also inconsistent with delaminated lower crustal melting.

Fractional crystallization (model 3) seems unlikely, as evidenced by small KQA major element variations (Fig. S3A and S3B), negligible Eu negative anomalies (Fig. S3C), and

no remarkable positive correlation between Sr/Y, $(Dy/Yb)_N$ (N—chondrite normalized), and SiO_2 (Fig. S5). An absence of substantial coeval mafic magma (Zhu et al., 2016; Hao et al., 2019) also does not support extensive fractional crystallization.

Lines of evidence indicate the KQAs have a subducted slab origin. The KQAs are similar to typical adakites (e.g., Drummond et al., 1996) in terms of their high SiO_2, Na_2O, Mg#, Sr/Y, and La/Yb (Castillo et al., 1999), and their mantle-like zircon $\delta^{18}O$ values (~5.5‰; Fig. 2C) are similar to those of oceanic slab–derived adakites (Bindeman et al., 2005). The high MgO and Mg# could have resulted from assimilation of mantle peridotite by slab melts (Rapp and Watson, 1995).

Nevertheless, variable amounts of continental crust must have been present in the source region of the KQAs. Their Sr-Nd isotope compositions and high Th/Ce and Th/La ratios (>0.3) (Figs. S6A and S6B) may have been inherited from continental crust instead of magma mixing, crustal assimilation, or sediment melting. An absence of mafic enclaves, hybrid schlieren (irregular streaks), and quenching textures (Fig. S1) excludes a magma mixing scenario. A slightly positive correlation between KQA Sr isotopes and MgO and no obvious correlation between $\varepsilon_{Nd(t)}$ and SiO_2 contents (Figs. S6C and S6D), combined with mantle-like zircon oxygen isotope compositions (Fig. 2C), argue against significant crustal contamination. Sediment melts have higher K_2O contents and K_2O/Na_2O ratios (Johnson and Plank, 2000) than the KQAs (Figs. S6E and S6F). In addition, the depleted Nd isotopic compositions of the KQAs contrast with those of subducted sediment–derived, ca. 162 Ma, high-Mg andesites (Fig. S4). Conversely, the KQAs have Pb isotope compositions marginally similar to those of the lower crust of the SQT (Li et al., 2016), which implies at least part of the continental crust signal could have been inherited from the overlying plate.

Constraints on Melting Conditions

Melting of a hydrated source is suggested for the formation of the KQAs based on the following evidence (Drummond et al., 1996; Prouteau et al., 1999). First, abundances of amphibole and biotite indicate high magma H_2O contents. Second, the Na_2O-rich character of the KQAs (Fig. 2A) is similar to that of trondhjemitic pegmatites, which originate as melts of garnet amphibolite under high aH_2O (activity of H_2O) (Sorensen, 1988). Their $Fe_2O_3^t$ (t—total) contents and CaO/Na_2O (Fig. S7) overlap those of melts of water-saturated basaltic rocks (Beard and Lofgren, 1991). Furthermore, the low zircon saturation temperatures (694–742 °C; Table S2) also reflect hydrated melting (Rapp and Watson, 1995). In addition, the high Sr/Y and Sr contents and weak Eu anomalies indicate the breakdown of plagioclase, consistent with the inferred high water content (Richards et al., 2012). Melting of hydrated source agrees with numerous experimental studies (Rapp and Watson, 1995; Prouteau et al., 1999) and a basalt ($aH_2O \geq 0.6$) solidus located between 650 and 800 °C at 1.0–3.5 GPa pressure range (Fig. 3A; Schmidt and Poli, 1998).

The KQAs were likely generated by partial melting of garnet amphibolite. Their Sr/Y arrays coincide with partial melts of mid-oceanic ridge basalt (MORB) with garnet amphibolite restite (Fig. 2B; Drummond et al., 1996). Their highest Sr/Y (up to 85) implies hydrous basalt melting pressures <2.5 GPa (Laurie and Stevens, 2012). Low HREE and Y contents and depletions in Nb and Ta (Fig. S3D) require garnet and rutile in the residue, which indicates a melting pressure of at least 1.5 GPa (e.g., Rapp and Watson, 1995; Xiong et al., 2011). Therefore, the applicable pressure-temperature conditions for slab melting are suggested to be at 1.5–2.5 GPa and 700–800 °C (Fig. 3A; Drummond et al., 1996).

Constraints on Subduction Erosion

The continental crust fingerprints and high H_2O content required for the generation of the KQAs could have been provided by hydrated forearc crust material. Descending slab devolatilizes efficiently in the shallow forearc region (Schmidt and Poli, 1998). This results in an increase of deep fluid overpressuring that may accentuate hydrofracturing, thus weakening the underside of the overriding plate and leading to locally enhanced subduction erosion (e.g., Bourgois et al., 1996). These hydrated and fragmented forearc crustal materials are carried by the descending slab into the deep mantle.

The KQAs are exposed <20 km north of the BNS (Fig. 1). Three potential factors may be responsible for their location relative to the BNS: (1) steep slab subduction, (2) crust shortening related to continental collision, or (3) forearc crust truncation associated with subduction erosion.

Hypothesis 1 seems implausible. Given the ~20 km arc-trench distance and the inferred 1.5–2.5 GPa melting pressure, the required slab dip angle would span >63° to 76°. Steep subduction does commonly occur where the subducted plate is old and cold enough. The age difference (~25 m.y.) between the KQAs (ca. 155 Ma) and MORBs of the BNS (ca. 180 Ma; Zhu et al., 2016), however, does not support such a hypothesis (Drummond et al., 1996). In fact, arc-trench distances >150 km commonly occur in active convergent margins even where the downgoing slab has a high dip angle (~80°; Dzierma et al., 2011).

Scenario 2 also appears to be implausible. First, no continent collision–related (ultra)high-pressure metamorphic rocks (e.g., eclogite) occur in the BNS, which indicates a soft collision (Zhu et al., 2016). Hence, limited crustal shortening is expected. Second, only ~90 km crustal shortening related to post-emplacement collision events in the Nyima area has been demonstrated (Kapp et al., 2007), but this is still not enough given typical arc-trench distances of >150 km. Third, the late Early Cretaceous SQT magma pulse has been explained by slab rollback (e.g., Hao et al., 2019). If true, then juxtaposition with the Jurassic arc would require additional shortening beyond that estimated to result from collision. Furthermore, the lack of deformation in the Kangqiong pluton (Fig. S1) also implies limited crust shortening.

Truncation of forearc crust resulting from subduction erosion (scenario 3) is supported by several lines of evidence. The significant ca. 175 Ma and ca. 154 Ma detrital zircon populations of SQT Jurassic sediments (Fig. S8) suggest intensive arc magmatism (Ma et al., 2017), yet coeval arc rocks are rare (e.g., Hao et al., 2019). Such a discrepancy implies arc consumption by subduction erosion. The Jurassic zircon content was reduced to <5% in the Cretaceous sediments (Fig. S8A). Similar observations have

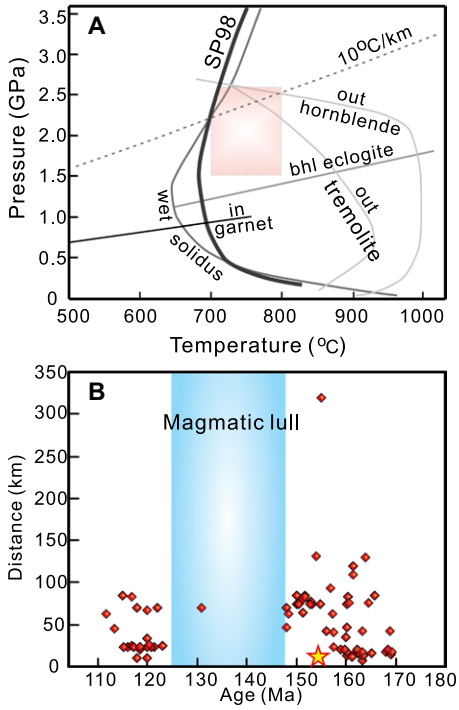

Figure 3. (A) Pressure-temperature (*P-T*) conditions for genesis of adakitic melts. Bold solid curve SP98 denotes solidus of water-saturated mid-oceanic ridge basalt; that curve and the garnet-in phase boundary are after Schmidt and Poli (1998); wet basalt solidus and others are after Drummond et al. (1996); dashed pink field is potential melting *P-T* space of Kangqiong adakites (KQAs; Tibet). (B) Perpendicular distance between Jurassic-Cretaceous arc rocks in the southern Qiangtang terrane and Bangong-Nujiang suture. Star shows KQAs. All cited age data are listed in Table S5 (see footnote 1).

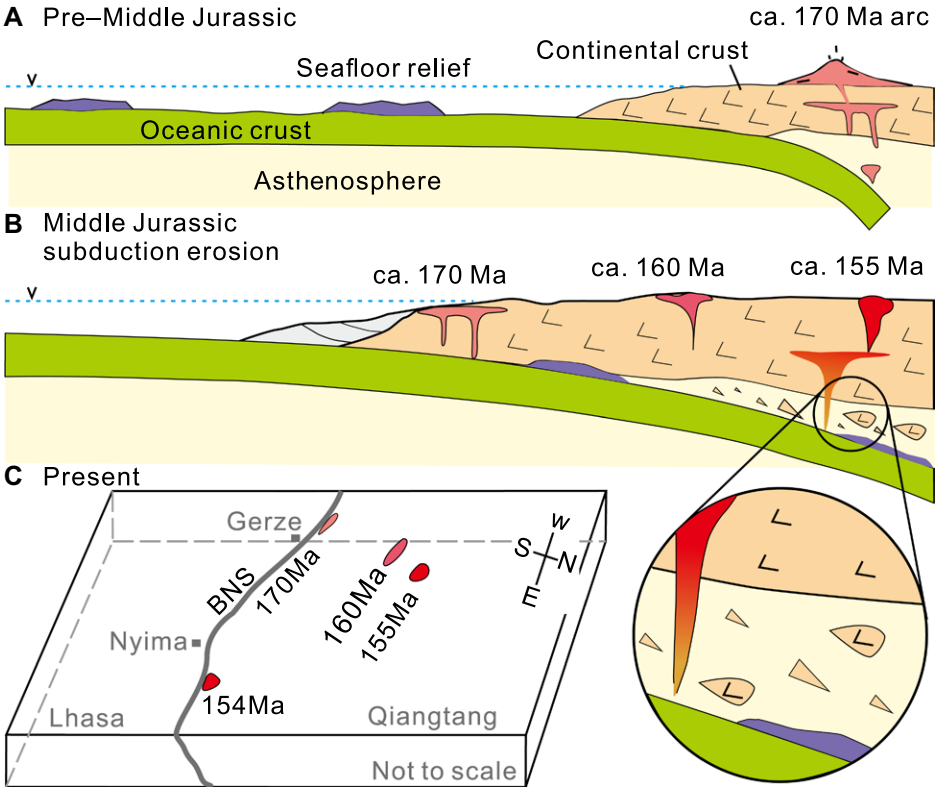

Figure 4. Cartoon of the subduction erosion model (modified after von Huene et al., 2004). (A) Generation of Middle Jurassic arc; positive topographic relief on the incoming slab could be a cause of later subduction erosion. (B) Forearc materials removed from the toe of the upper plate have been involved in arc source melting, which was accompanied by forearc crust truncation and frontal-arc migration toward the hinterland. (C) Observed short arc-suture distance could be a consequence of subduction erosion. BNS—Bangong-Nujiang suture.

been attributed to consumption of an early arc due to subduction erosion (Grove et al., 2008). Secondly, the ca. 174–168 Ma rapid subsidence in the SQT forearc basin, from shallow-marine limestone to deep-sea turbidite depositional environments (Ma et al., 2017), is also compatible with crustal thinning associated with subduction erosion (Kopp et al., 2006; Vannucchi et al., 2013). Finally, subduction erosion is invoked to explain the ca. 177 Ma high-pressure granulite metamorphism (Zhang et al., 2017).

Whereas active-spreading-ridge subduction seems unlikely, given the absence of coeval SQT high-Mg andesites, A-type granites, and ocean island basalt–like rocks (Hao et al., 2019), the spatial and temporal relationships in the Jurassic arc (Fig. 3B) are consistent with subduction erosion (Fig. 4). Migration of the Jurassic arc front toward the continental interior and the following magmatic lull can be reconciled by subduction of buoyant crust and positive relief on the oceanic slab (e.g., Kay et al., 2005; Goss et al., 2013); e.g., an oceanic plateau (Hao et al., 2019). Similar events generated the late Cenozoic adakite-like andesites in the Chilean-Pampean flat-slab subduction zone (Goss et al., 2013). Subduction of these major topographic anomalies not only narrowed the mantle wedge (it ultimately disappeared), and ended arc magmatism (Fig. 3B; Kay et al., 2005; Goss et al., 2013), but also resulted in forearc retreat as indicated by a narrow arc-trench gap (Kopp et al., 2006).

IMPLICATIONS

In the fossil BNS, central Tibet, the anomalously short arc-suture distance combined with arc frontal migration and other independent geological observations can be explained well by a subduction erosion model. The present case has provided the first solid magmatic evidence for crustal mass recycling by subduction erosion in a fossil subduction zone. Given the Cenozoic cases from active subduction zones (Bourgois et al., 1996; von Huene et al., 2004; Kopp et al., 2006; Goss et al., 2013), we suggest that subduction erosion is commonplace and has been important for crustal material recycling since the initiation of slab subduction beneath continents.

ACKNOWLEDGMENTS

The manuscript was improved by constructive suggestions from editor Chris Clark and two anonymous reviewers. Financial support was provided by the Second Tibetan Plateau Scientific Expedition and Research (STEP) (grant 2019QZKK0702) and the National Natural Science Foundation of China (grants 91855215, 41630208, and 42021002). This is contribution 2964 of the Guangzhou Institute of Geochemistry, Chinese Academy of Sciences (GIGCAS).

REFERENCES CITED

Beard, J.S., and Lofgren, G.E., 1991, Dehydration melting and water-saturated melting of basaltic and andesitic greenstones and amphibolites at 1, 3, and 6.9 kb: Journal of Petrology, v. 32, p. 365–401, https://doi.org/10.1093/petrology/32.2.365.

Bindeman, I.N., Eiler, J.M., Yogodzinski, G.M., Tatsumi, Y., Stern, C.R., Grove, T.L., Portnyagin, M., Hoernle, K., and Danyushevsky, L.V., 2005, Oxygen isotope evidence for slab melting in modern and ancient subduction zones: Earth and Planetary Science Letters, v. 235, p. 480–496, https://doi.org/10.1016/j.epsl.2005.04.014.

Bourgois, J., Martin, H., Lagabrielle, Y., Le Moigne, J., and Jara, J.F., 1996, Subduction erosion related to spreading-ridge subduction: Taitao peninsula (Chile margin triple junction area): Geology, v. 24, p. 723–726, https://doi.org/10.1130/0091-7613(1996)024<0723:SERTSR>2.3.CO;2.

Cao, Y., Sun, Z., Li, H., Ye, X., Pan, J., Liu, D., Zhang, L., Wu, B., Cao, X., Liu, C., and Yang, Z., 2020, Paleomagnetism and U-Pb geochronology of Early Cretaceous volcanic rocks from the Qiangtang Block, Tibetan Plateau: Implications for the Qiangtang-Lhasa collision: Tectonophysics, v. 789, 228500, https://doi.org/10.1016/j.tecto.2020.228500.

Castillo, P.R., Janney, P.E., and Solidum, R.U., 1999, Petrology and geochemistry of Camiguin Island, southern Philippines: Insights to the source of adakites and other lavas in a complex arc setting: Contributions to Mineralogy and Petrology, v. 134, p. 33–51, https://doi.org/10.1007/s004100050467.

Clift, P.D., Vannucchi, P., and Morgan, J.P., 2009, Crustal redistribution, crust-mantle recycling and Phanerozoic evolution of the continental crust: Earth-Science Reviews, v. 97, p. 80–104, https://doi.org/10.1016/j.earscirev.2009.10.003.

Drummond, M.S., Defant, M.J., and Kepezhinskas, P.K., 1996, Petrogenesis of slab-derived trondhjemite–tonalite–dacite/adakite magmas: Earth and Environmental Science Transactions of the Royal Society of Edinburgh, v. 87, p. 205–215, https://doi.org/10.1017/S0263593300006611.

Dzierma, Y., Rabbel, W., Thorwart, M.M., Flueh, E.R., Mora, M.M., and Alvarado, G.E., 2011, The steeply subducting edge of the Cocos Ridge: Evidence from receiver functions beneath the northern Talamanca Range, south-central Costa Rica: Geochemistry Geophysics Geosystems, v. 12, Q04S30, https://doi.org/10.1029/2010GC003477.

Goss, A.R., Kay, S.M., and Mpodozis, C., 2013, Andean adakite-like high-Mg andesites on the northern margin of the Chilean-Pampean flat-slab (27–28.5°S) associated with frontal arc migration and fore-arc subduction erosion: Journal of Petrology, v. 54, p. 2193–2234, https://doi.org/10.1093/petrology/egt044.

Grove, M., Bebout, G.E., Jacobson, C.E., Barth, A.P., Kimbrough, D.L., King, R.L., Zou, H., Lovera, O.M., Mahoney, B.J., and Gehrels, G.E., 2008, The Catalina Schist: Evidence for middle Cretaceous subduction erosion of southwestern North America, *in* Draut, A.E., et al., eds., Formation and Applications of the Sedimentary Record in Arc Collision Zones: Geological Society of America Special Paper 436, p. 335–361, https://doi.org/10.1130/2008.2436(15).

Hao, L.-L., Wang, Q., Zhang, C., Ou, Q., Yang, J.-H., Dan, W., and Jiang, Z.-Q., 2019, Oceanic plateau subduction during closure of the

Bangong-Nujiang Tethyan Ocean: Insights from central Tibetan volcanic rocks: Geological Society of America Bulletin, v. 131, p. 864–880, https://doi.org/10.1130/B32045.1.

Johnson, M.C., and Plank, T., 2000, Dehydration and melting experiments constrain the fate of subducted sediments: Geochemistry Geophysics Geosystems, v. 1, 1007, https://doi.org/10.1029/1999GC000014.

Kapp, P., and DeCelles, P.G, 2019, Mesozoic–Cenozoic geological evolution of the Himalayan-Tibetan orogen and working tectonic hypotheses: American Journal of Science, v. 319, p. 159–254, https://doi.org/10.2475/03.2019.01.

Kapp, P., DeCelles, P.G., Gehrels, G.E., Heizler, M., and Ding, L., 2007, Geological records of the Lhasa-Qiangtang and Indo-Asian collisions in the Nima area of central Tibet: Geological Society of America Bulletin, v. 119, p. 917–933, https://doi.org/10.1130/B26033.1.

Kay, S.M., Godoy, E., and Kurtz, A., 2005, Episodic arc migration, crustal thickening, subduction erosion, and magmatism in the south-central Andes: Geological Society of America Bulletin, v. 117, p. 67–88, https://doi.org/10.1130/B25431.1.

Kopp, H., Flueh, E.R., Petersen, C.J., Weinrebe, W., Wittwer, A., and Meramex Scientists, 2006, The Java margin revisited: Evidence for subduction erosion off Java: Earth and Planetary Science Letters, v. 242, p. 130–142, https://doi.org/10.1016/j.epsl.2005.11.036.

Lai, W., Hu, X., Garzanti, E., Xu, Y., Ma, A., and Li, W., 2019, Early Cretaceous sedimentary evolution of the northern Lhasa terrane and the timing of initial Lhasa-Qiangtang collision: Gondwana Research, v. 73, p. 136–152, https://doi.org/10.1016/j.gr.2019.03.016.

Laurie, A., and Stevens, G., 2012, Water-present eclogite melting to produce Earth's early felsic crust: Chemical Geology, v. 314–317, p. 83–95, https://doi.org/10.1016/j.chemgeo.2012.05.001.

Li, Y., He, J., Han, Z., Wang, C., Ma, P., Zhou, A., Liu, S.-A., and Xu, M., 2016, Late Jurassic sodium-rich adakitic intrusive rocks in the southern Qiangtang terrane, central Tibet, and their implications for the Bangong-Nujiang Ocean subduction: Lithos, v. 245, p. 34–46, https://doi.org/10.1016/j.lithos.2015.10.014.

Ma, A., Hu, X., Garzanti, E., Han, Z., and Lai, W., 2017, Sedimentary and tectonic evolution of the southern Qiangtang basin: Implications for the Lhasa-Qiangtang collision timing: Journal of Geophysical Research: Solid Earth, v. 122, p. 4790–4813, https://doi.org/10.1002/2017JB014211.

Prouteau, G., Scaillet, B., Pichavant, M., and Maury, R.C., 1999, Fluid-present melting of ocean crust in subduction zones: Geology, v. 27, p. 1111–1114, https://doi.org/10.1130/0091-7613(1999)027<1111:FPMOOC>2.3.CO;2.

Ranero, C.R., and von Huene, R., 2000, Subduction erosion along the Middle America convergent margin: Nature, v. 404, p. 748–752, https://doi.org/10.1038/35008046.

Rapp, R.P., and Watson, E.B., 1995, Dehydration melting of metabasalt at 8–32 kbar: Implications for continental growth and crust-mantle recycling: Journal of Petrology, v. 36, p. 891–931, https://doi.org/10.1093/petrology/36.4.891.

Richards, J.P., Spell, T., Rameh, E., Razique, A., and Fletcher, T., 2012, High Sr/Y magmas reflect arc maturity, high magmatic water content, and porphyry Cu ± Mo ± Au potential: Examples from the Tethyan arcs of central and eastern Iran and western Pakistan: Economic Geology and the Bulletin of the Society of Economic Geologists, v. 107, p. 295–332, https://doi.org/10.2113/econgeo.107.2.295.

Schmidt, M.W., and Poli, S., 1998, Experimentally based water budgets for dehydrating slabs and consequences for arc magma generation: Earth and Planetary Science Letters, v. 163, p. 361–379, https://doi.org/10.1016/S0012-821X(98)00142-3.

Scholl, D.W., von Huene, R., Vallier, T.L., and Howell, D.G., 1980, Sedimentary masses and concepts about tectonic processes at underthrust ocean margins: Geology, v. 8, p. 564–568, https://doi.org/10.1130/0091-7613(1980)8<564:SMACAT>2.0.CO;2.

Sorensen, S.S., 1988, Petrology of amphibolite-facies mafic and ultramafic rocks from the Catalina Schist, southern California: Metasomatism and migmatization in a subduction zone metamorphic setting: Journal of Metamorphic Geology, v. 6, p. 405–435, https://doi.org/10.1111/j.1525-1314.1988.tb00431.x.

Stern, C.R., and Kilian, R., 1996, Role of the subducted slab, mantle wedge and continental crust in the generation of adakites from the Andean Austral Volcanic Zone: Contributions to Mineralogy and Petrology, v. 123, p. 263–281, https://doi.org/10.1007/s004100050155.

Straub, S.M., Gómez-Tuena, A., and Vannucchi, P., 2020, Subduction erosion and arc volcanism: Nature Reviews Earth & Environment, v. 1, p. 574–589, https://doi.org/10.1038/s43017-020-0095-1.

Vannucchi, P., Sak, P.B., Morgan, J.P., Ohkushi, K.i., Ujiie, K., and the IODP Expedition 334 Shipboard Scientists, 2013, Rapid pulses of uplift, subsidence, and subduction erosion offshore Central America: Implications for building the rock record of convergent margins: Geology, v. 41, p. 995–998, https://doi.org/10.1130/G34355.1.

von Huene, R., Ranero, C.R., and Vannucchi, P., 2004, Generic model of subduction erosion: Geology, v. 32, p. 913–916, https://doi.org/10.1130/G20563.1.

Wang, Q., et al., 2008, Eocene melting of subducting continental crust and early uplifting of central Tibet: Evidence from central-western Qiangtang high-K calc-alkaline andesites, dacites and rhyolites: Earth and Planetary Science Letters, v. 272, p. 158–171, https://doi.org/10.1016/j.epsl.2008.04.034.

Xiong, X., Keppler, H., Audétat, A., Ni, H., Sun, W., and Li, Y., 2011, Partitioning of Nb and Ta between rutile and felsic melt and the fractionation of Nb/Ta during partial melting of hydrous metabasalt: Geochimica et Cosmochimica Acta, v. 75, p. 1673–1692, https://doi.org/10.1016/j.gca.2010.06.039.

Zhang, X.-Z., Wang, Q., Dong, Y.-S., Zhang, C., Li, Q.-Y., Xia, X.-P., and Xu, W., 2017, High-pressure granulite facies overprinting during the exhumation of eclogites in the Bangong-Nujiang suture zone, central Tibet: Link to flat-slab subduction: Tectonics, v. 36, p. 2918–2935, https://doi.org/10.1002/2017TC004774.

Zhu, D.-C., Li, S.-M., Cawood, P.A., Wang, Q., Zhao, Z.-D., Liu, S.-A., and Wang, L.-Q., 2016, Assembly of the Lhasa and Qiangtang terranes in central Tibet by divergent double subduction: Lithos, v. 245, p. 7–17, https://doi.org/10.1016/j.lithos.2015.06.023.

Printed in USA